J. Fluid Mech. (1991), *vol.* 227, *pp.* 193–209
Printed in Great Britain

Visual observations of the flow around a half-submerged oscillating sphere

By SADATOSHI TANEDA
Kurume Institute of Technology, Kamitsu, Kurume 830, Japan

(Received 9 September 1990)

Visual observations are made on the flow around a sphere which is half-submerged in still water and forced to oscillate up and down. It is found that three kinds of steady flows are generated in the water: the surface flow, the undersurface flow, and the vertical jet flow. The surface flow is produced in the very thin layer on the water surface. The undersurface flow is induced in the thick layer under the water surface. The vertical jet flow is ejected vertically from the bottom of the sphere. The surface flow and the undersurface flow are produced only when petal-shaped waves are generated on the water surface. The velocity of the undersurface flow is much smaller than that of the surface flow.

1. Introduction

Petal-shaped waves are generated around a sphere which is half-submerged in water and forced to oscillate vertically, provided that either the frequency or the amplitude is large (Okabe & Inoue 1967; Tatsuno, Inoue & Okabe 1969; Taneda 1986). So far as we know, however, no observations have yet been made on the flow induced in the water. The purpose of the present experiments is to determine the flow structure using flow visualization techniques.

2. Apparatus and experimental method

Figure 1 shows a schematic diagram of the apparatus used in the present experiments. The glass water tank was 60 cm in length, 30 cm in width and 36 cm in depth. The depth of the water was fixed at 13 cm. A plastic sphere 3.8 cm in diameter was used as the test sphere. The oscillation amplitude of the sphere was varied from 0.1 mm to 2.5 mm. All the experiments were carried out at a frequency of 30 Hz. For flow visualization, aluminium flakes were used as the tracer particles. In order to keep the water surface clean, a few droplets of detergent were added into the water. The surface tension of the water used in the present experiment was about 40 dyn/cm.

3. Results

Figure 2 shows the wave patterns at various oscillation amplitudes. When the oscillation amplitude of the sphere $a < 0.50$ mm (figure 2*a*), concentric circular waves whose frequency is the same as that of sphere motion are generated on the water surface. The wavelength is 6.9 mm, and the wave velocity is 21 cm/s. When $a > 0.50$ mm (figure 2*b*), standing cross-waves whose frequency is one half that of the sphere motion are superimposed on the concentric circular waves. As a result, a petal-

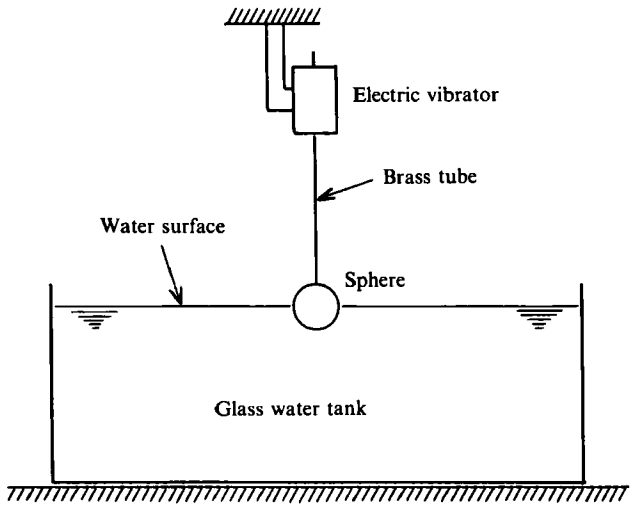

FIGURE 1. Schematic diagram of the experimental apparatus.

shaped wave pattern is formed on the water surface. The petal-shaped waves are 15 Hz in frequency and 13.8 mm in wavelength. The wave pattern is regular when $a < 1.0$ mm (figure 2*c*), but becomes irregular at about $a = 1.0$ mm (figure 2*d*). The irregularity of the wave pattern increases with the oscillation amplitude (figure 2*e*, *f*).

Figure 3 shows the variation of the surface flow with the oscillation amplitude. To make the surface flow visible, the water surface is scattered with aluminium flakes. No surface flow exists when concentric circular waves are generated on the water surface (figure 3*a*). Surface flows make their appearance, however, when petal-shaped waves are generated on the water surface (figure 3*b*–*h*). It will be seen that the surface flow consists of many recirculating flows. The region where the surface flow exists spreads as the oscillation amplitude is increased. The surface flow is very sensitive to external disturbances, so that the arrangement of the recirculating flows is rarely symmetrical.

Figure 4 shows the undersurface flows at various oscillation amplitudes, visualized with aluminium flakes suspended uniformly in the water. The horizontal layer close to the water surface is illuminated with a 500 W projector. The illuminated layer of about 5 mm thickness does not extend up to the water surface, but stops short of the region where the waves gives an up-and-down motion to the surface. When $a < 0.5$ mm, no undersurface flow can be seen (figure 4*a*). When $0.5 \text{ mm} < a < 1.0$ mm, however, regular undersurface flows are induced (figure 4*b*, *c*). Transition from laminar to turbulent flow takes place at about $a = 1.0$ mm (figure 4*d*). The intensity of turbulence increases with the oscillation amplitude (figure 4*e*, *f*). It can be seen from figures 3 and 4 that the velocity of the undersurface flow is much smaller than that of the surface flow.

Figure 5 shows the flow in a vertical plane containing the centre of the sphere. The illuminated layer is 6 mm in thickness. As will be seen, a vertical jet flow is ejected from the bottom of the sphere. The length of the jet flow increases with the oscillation amplitude (figure 5*a*–*c*). Transition from laminar to turbulent flow occurs at about $a = 2$ mm (figure 5*d*). Figure 6 shows a closeup of the flow at $a = 0.75$ mm. We find

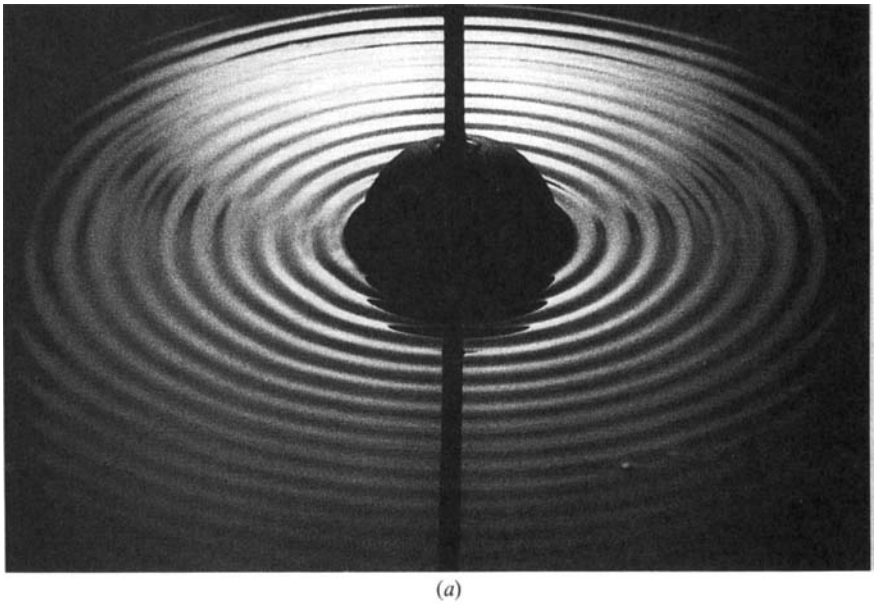

(*a*)

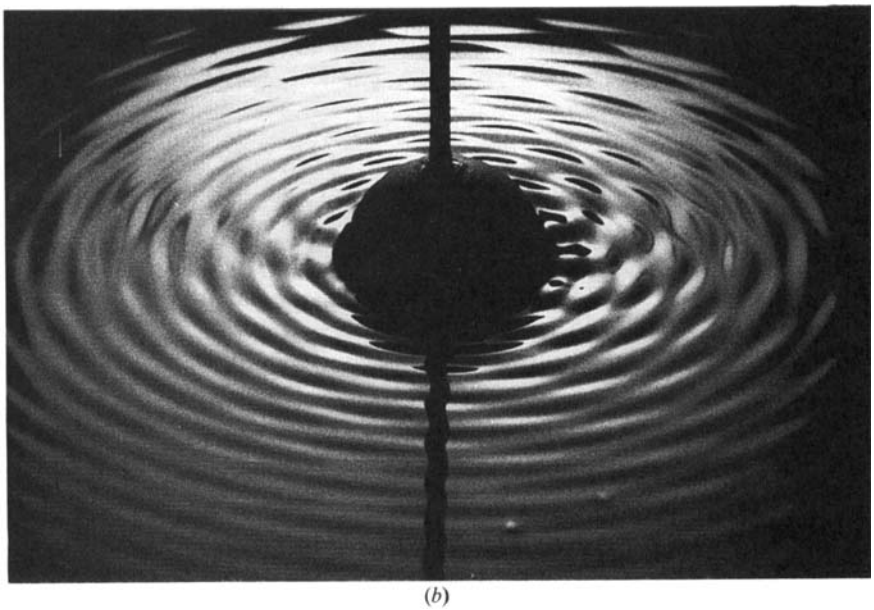

(*b*)

FIGURE 2(*a*, *b*). For caption see p. 197.

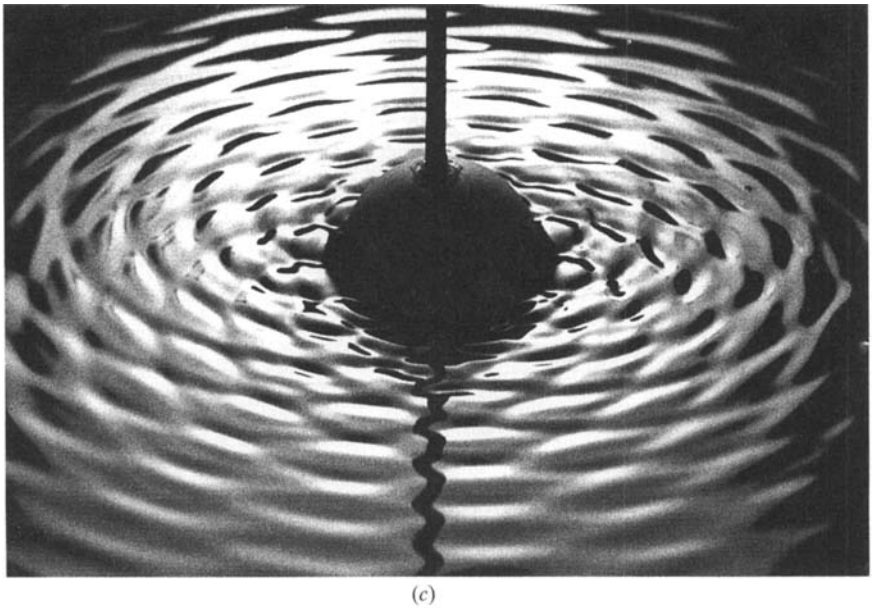

(c)

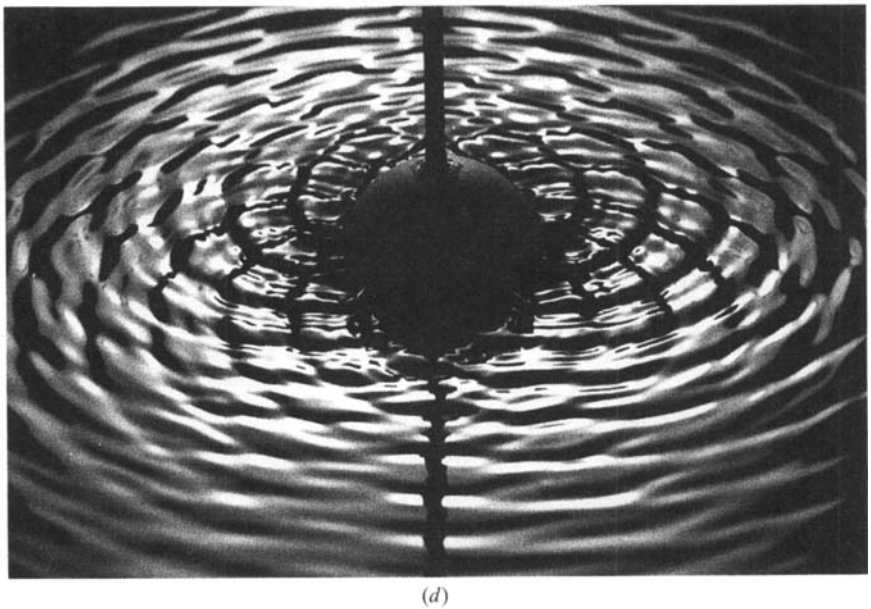

(d)

FIGURE 2(c, d). For caption see facing page.

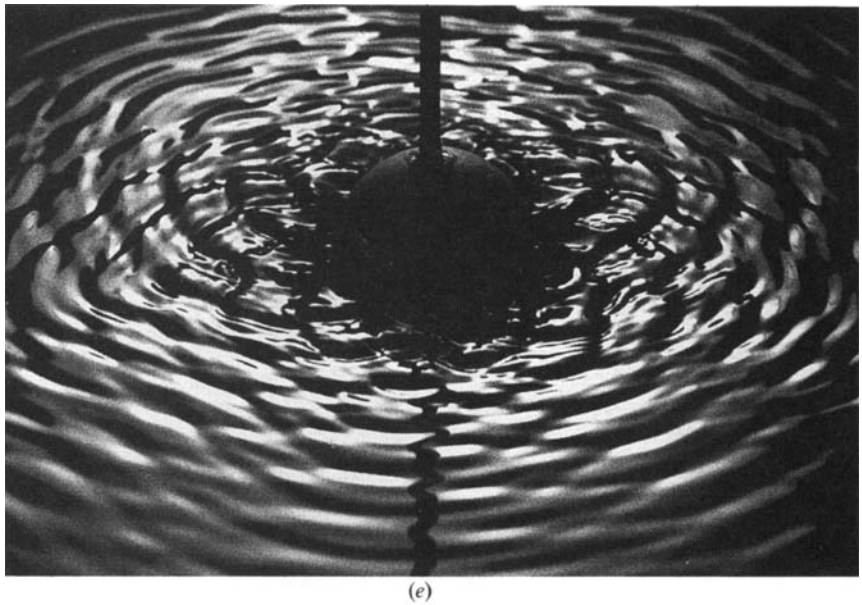

(*e*)

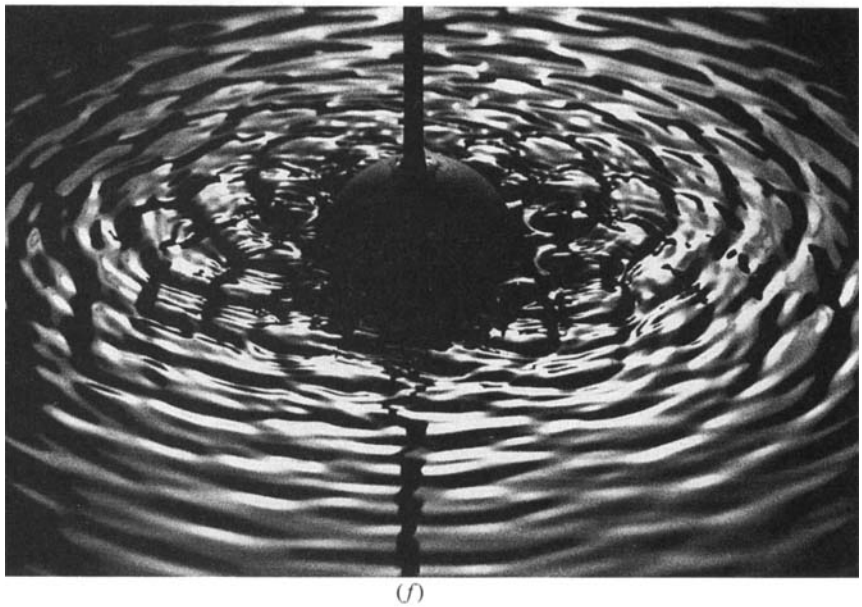

(*f*)

FIGURE 2. Wave patterns: (*a*) $a = 0.45$ mm; (*b*) 0.52 mm; (*c*) 0.69 mm; (*d*) 1.05 mm; (*e*) 1.33 mm; (*f*) 1.68 mm. (Time of exposure is 0.001 s; elapsed time from initiation of the sphere's oscillation is 30 s.)

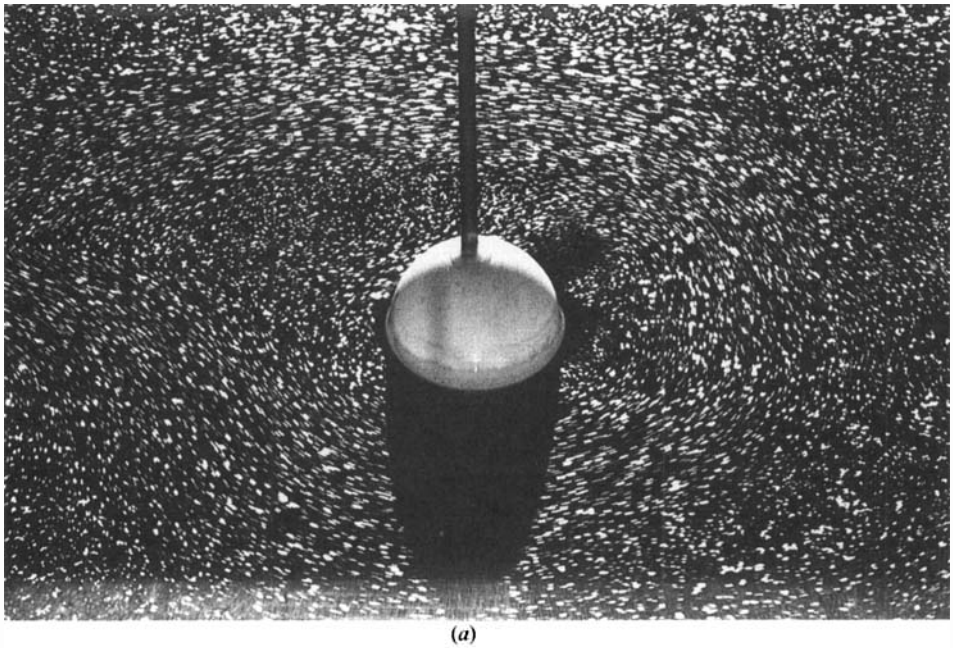

(*a*)

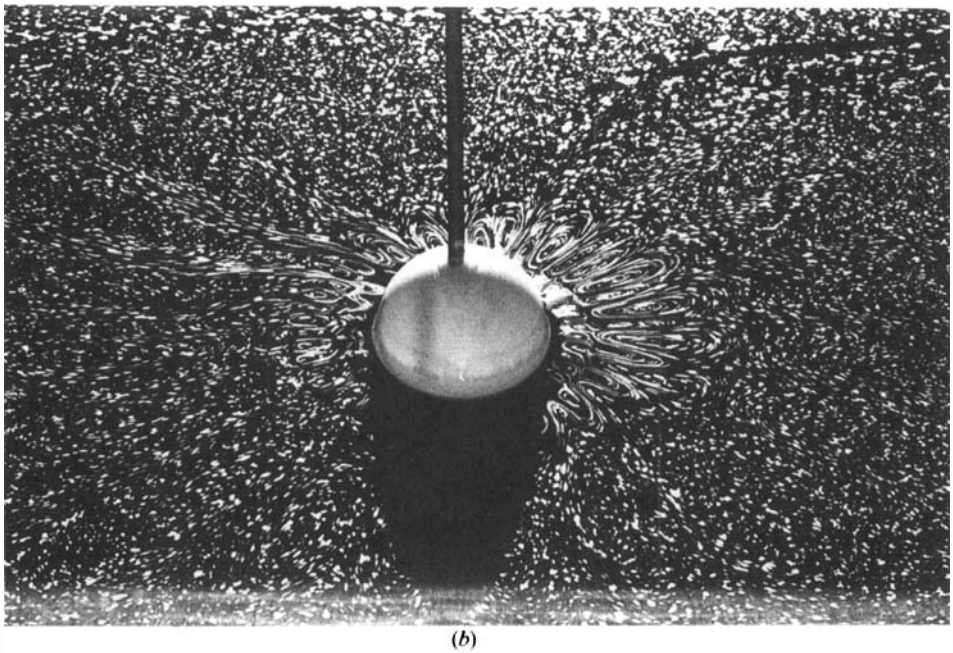

(*b*)

FIGURE 3 (*a*, *b*). For caption see p. 201.

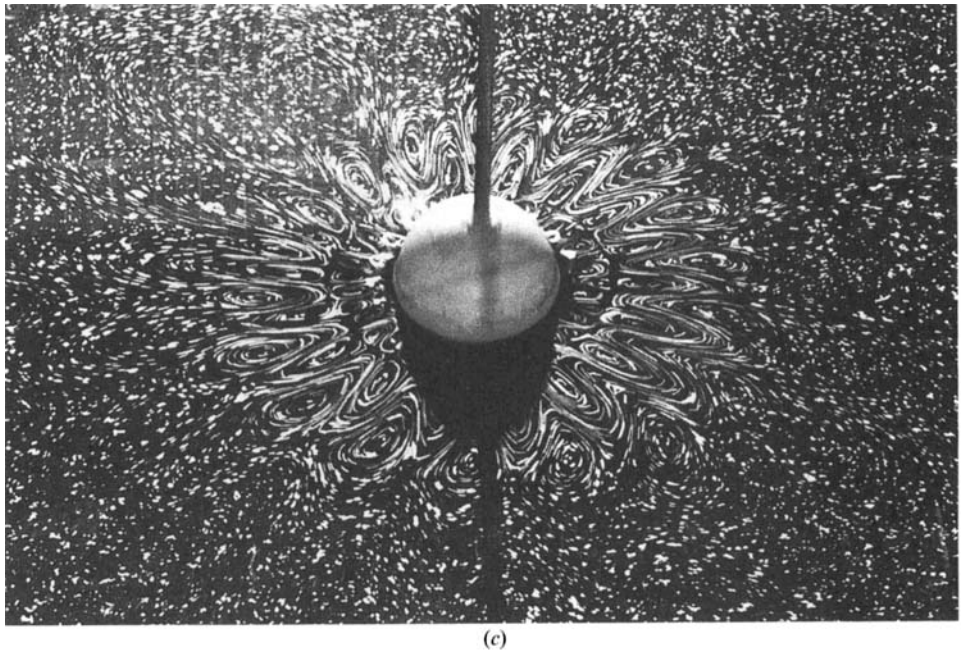

(*c*)

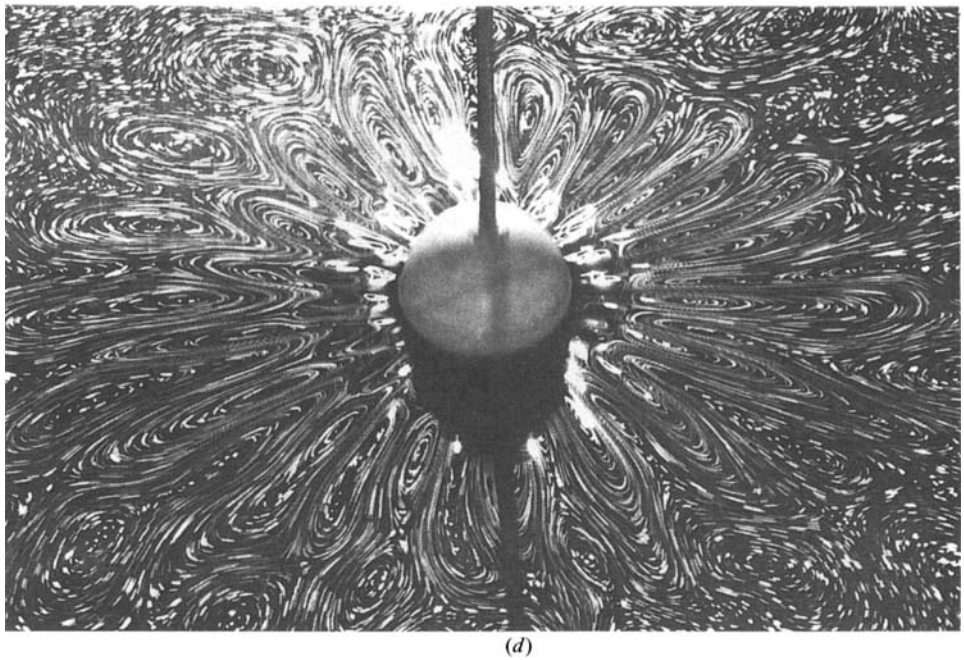

(*d*)

FIGURE 3(*c*, *d*). For caption see p. 201.

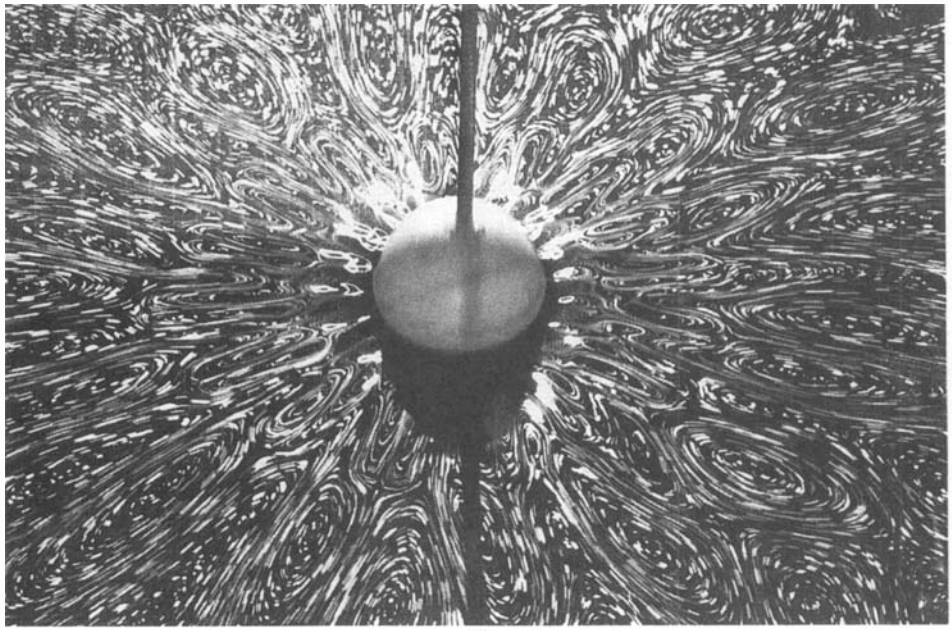

(e)

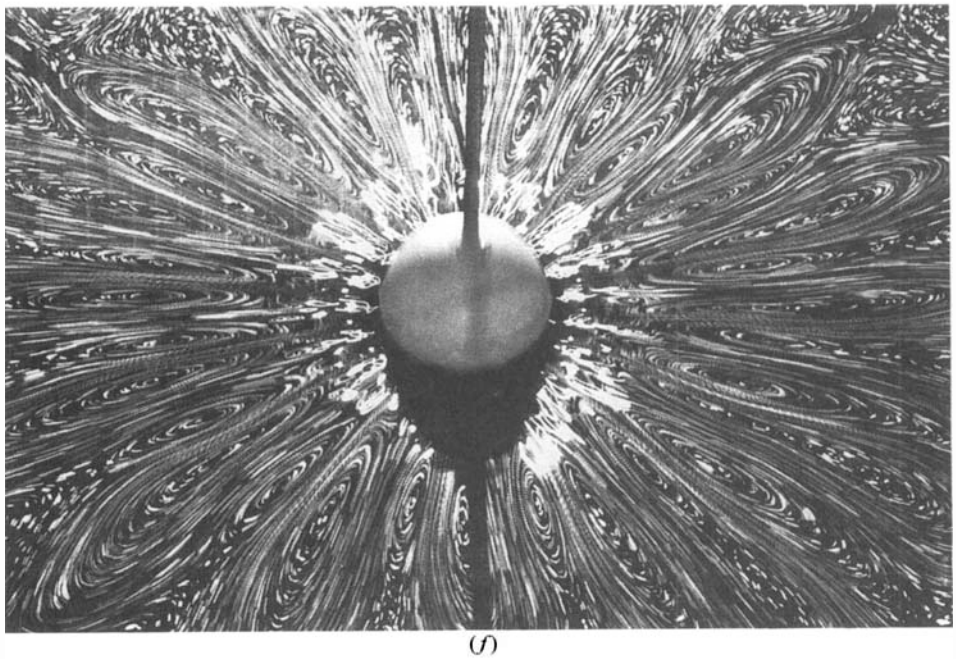

(f)

FIGURE 3(e, f). For caption see facing page.

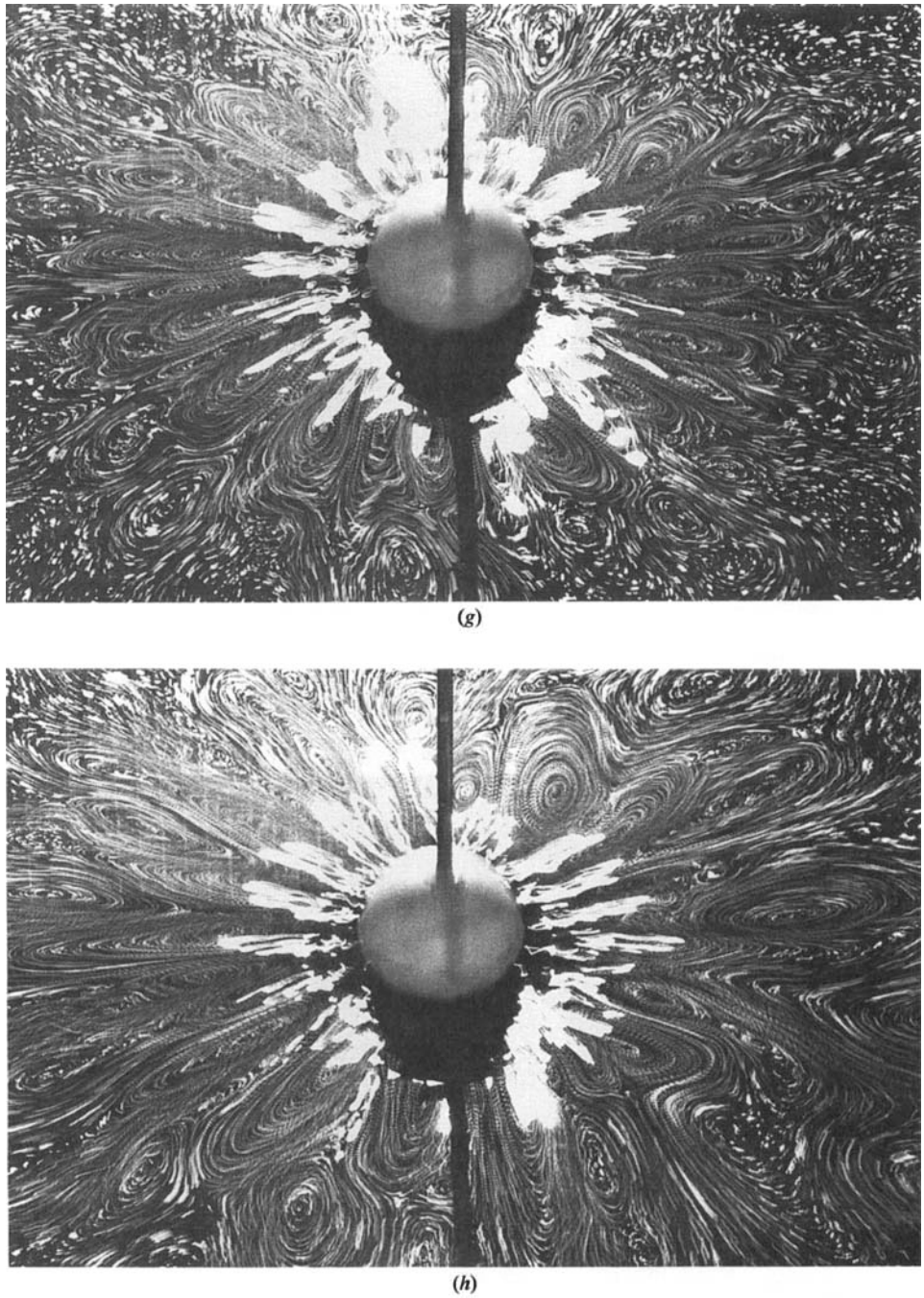

FIGURE 3. Surface flows: (*a*) $a = 0.50$ mm; (*b*) 0.58 mm; (*c*) 0.75 mm; (*d*) 0.95 mm; (*e*) 1.10 mm; (*f*) 1.35 mm; (*g*) 1.60 mm; (*h*) 1.85 mm. (Time of exposure is 1 s; elapsed time from initiation of the sphere's oscillation is 30 s.)

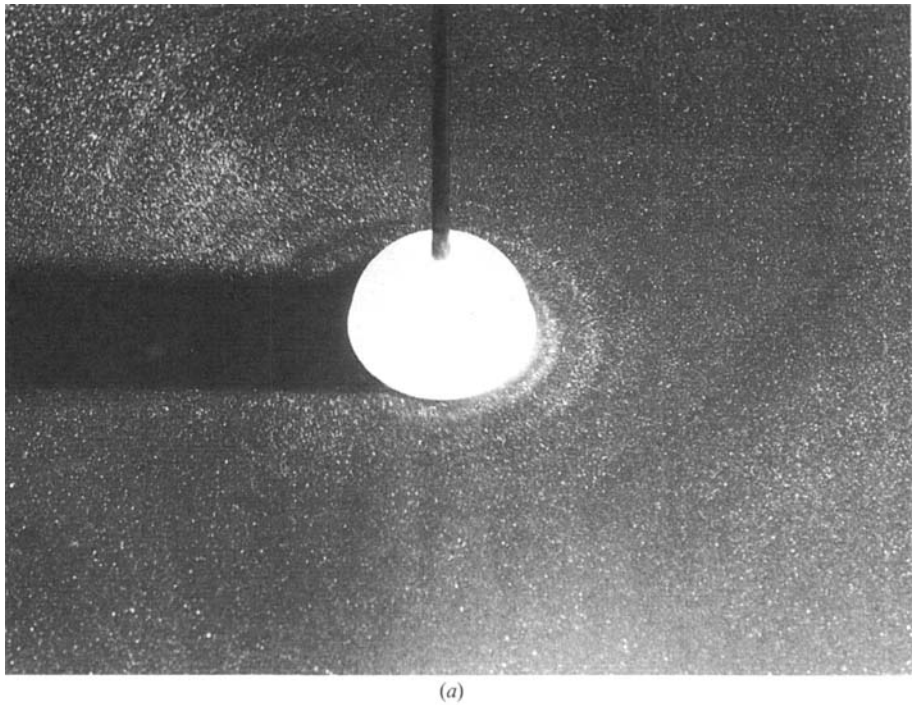

(*a*)

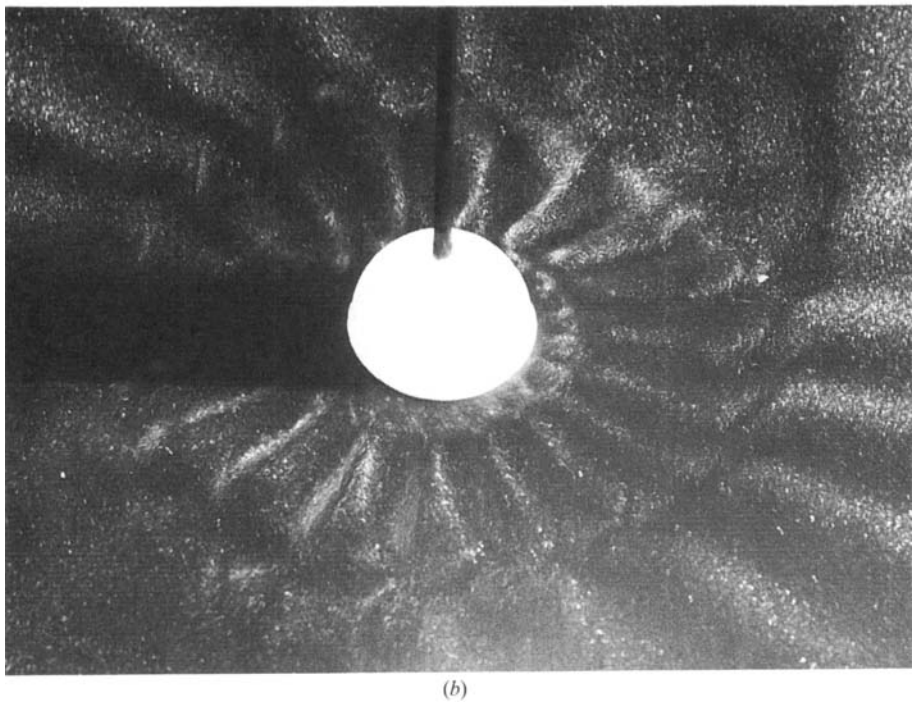

(*b*)

FIGURE 4(*a*, *b*). For caption see p. 204.

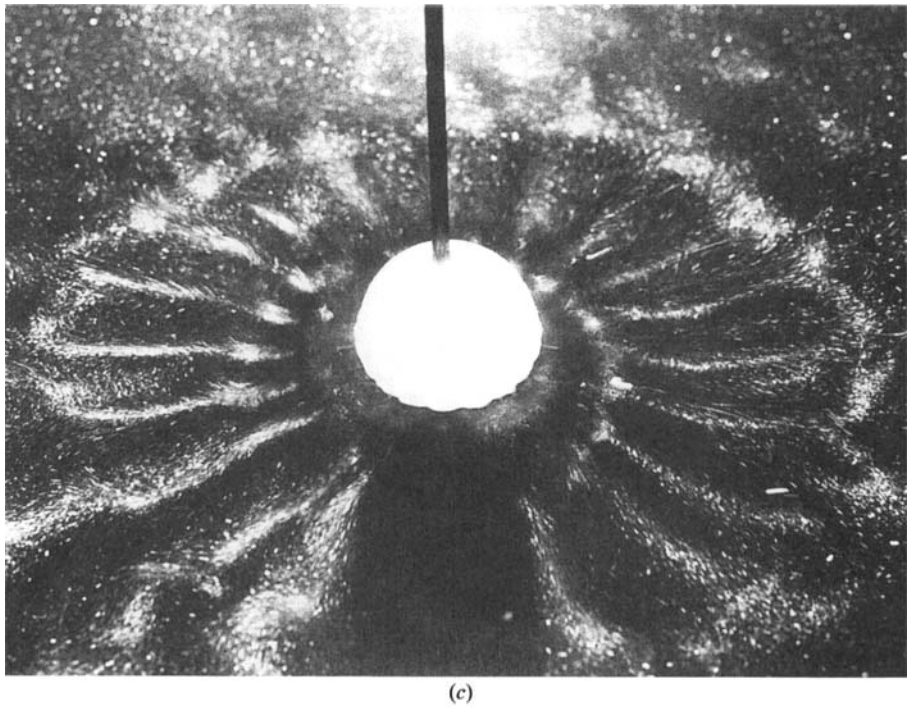

(*c*)

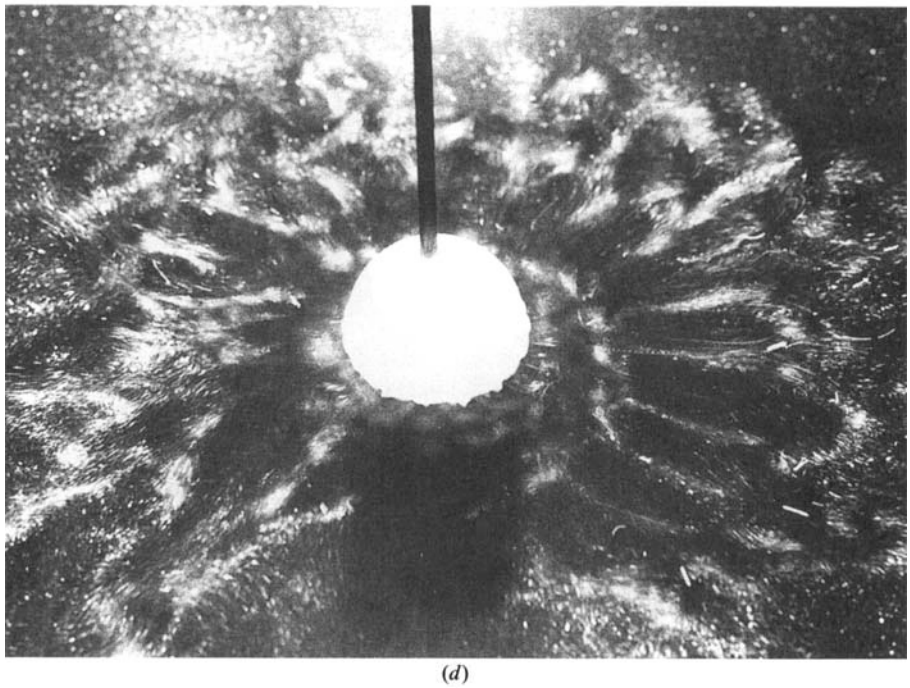

(*d*)

FIGURE 4(*c*, *d*). For caption see page 204.

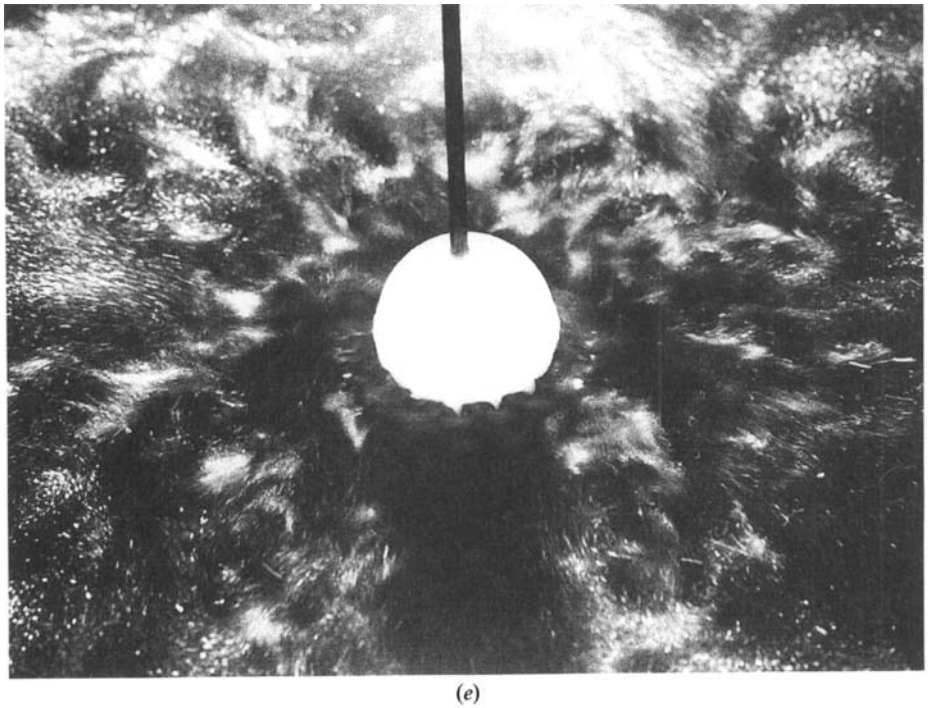

(e)

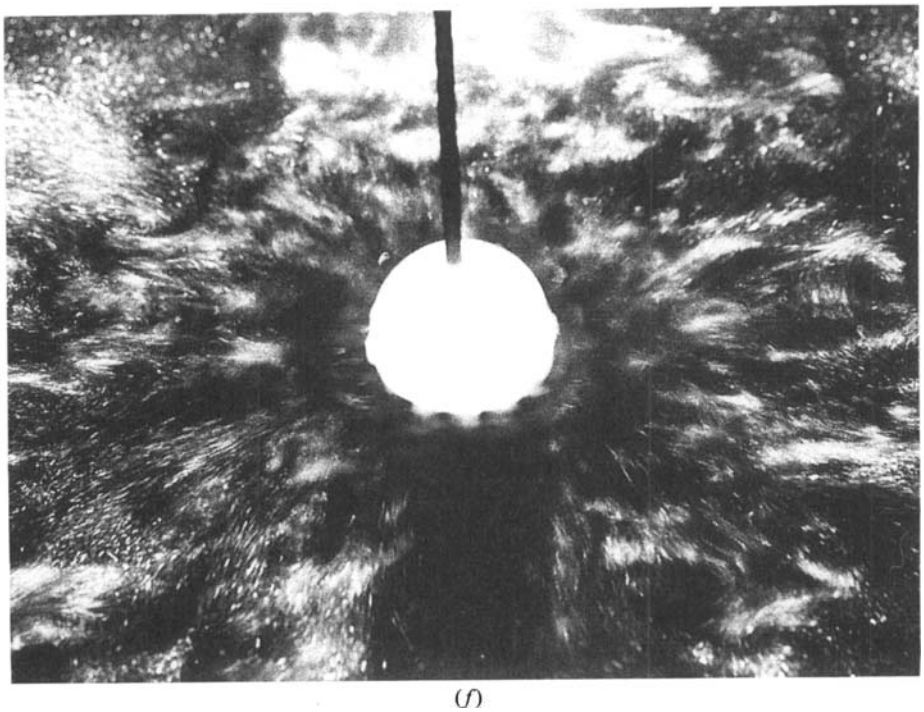

(f)

FIGURE 4. Undersurface flows: (a) $a = 0.50$ mm; (b) 0.60 mm; (c) 0.79 mm; (d) 0.99 mm; (e) 1.20 mm; (f) 1.75 mm. (Time of exposure is 1 s; elapsed time from initiation of the sphere oscillation is 30 s.)

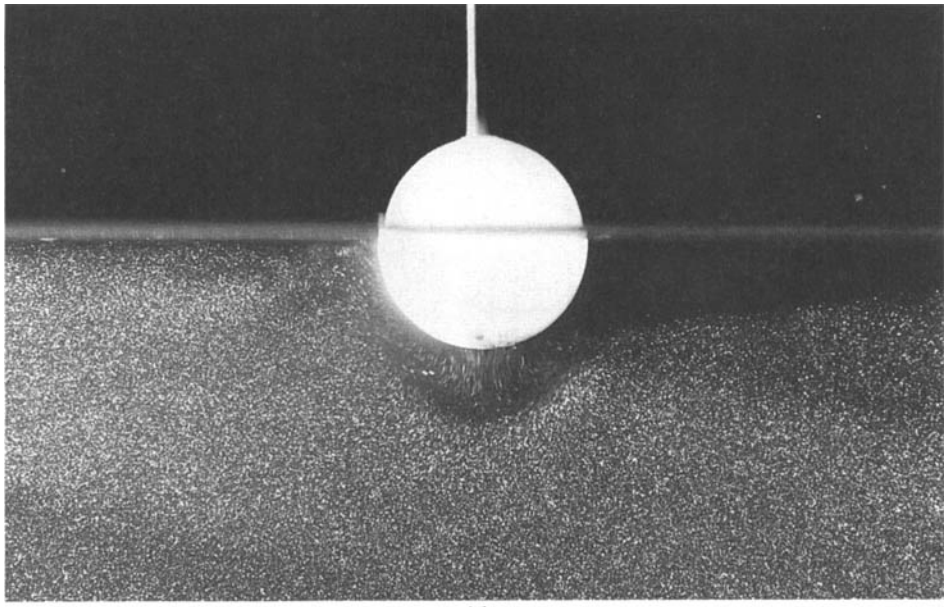

(*a*)

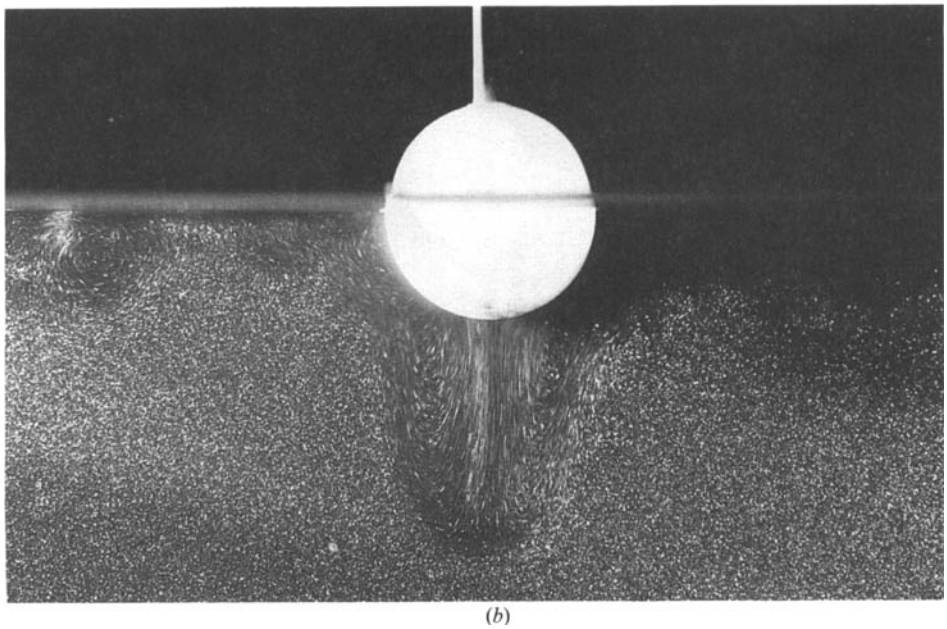

(*b*)

FIGURE 5(*a*, *b*). For caption see p. 206.

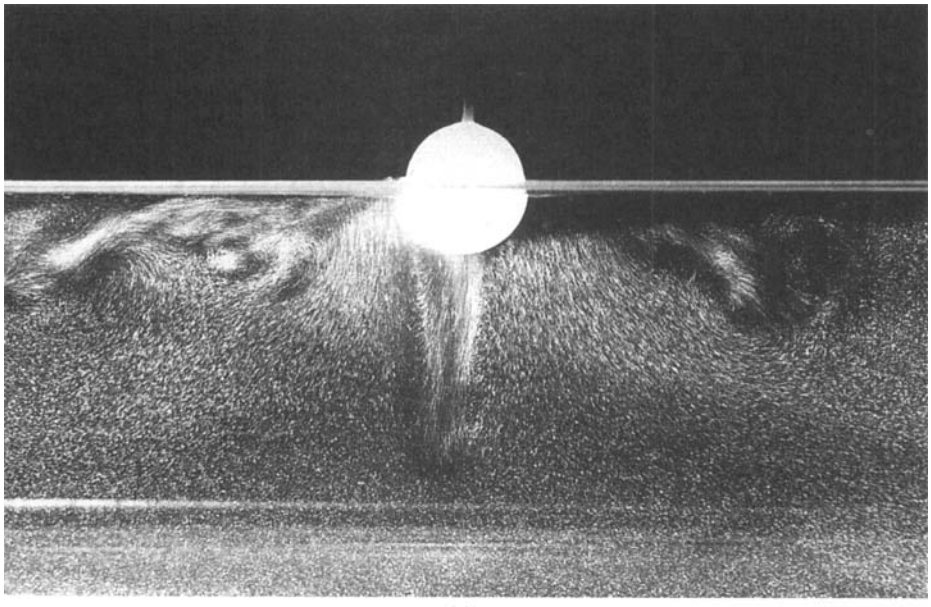

(c)

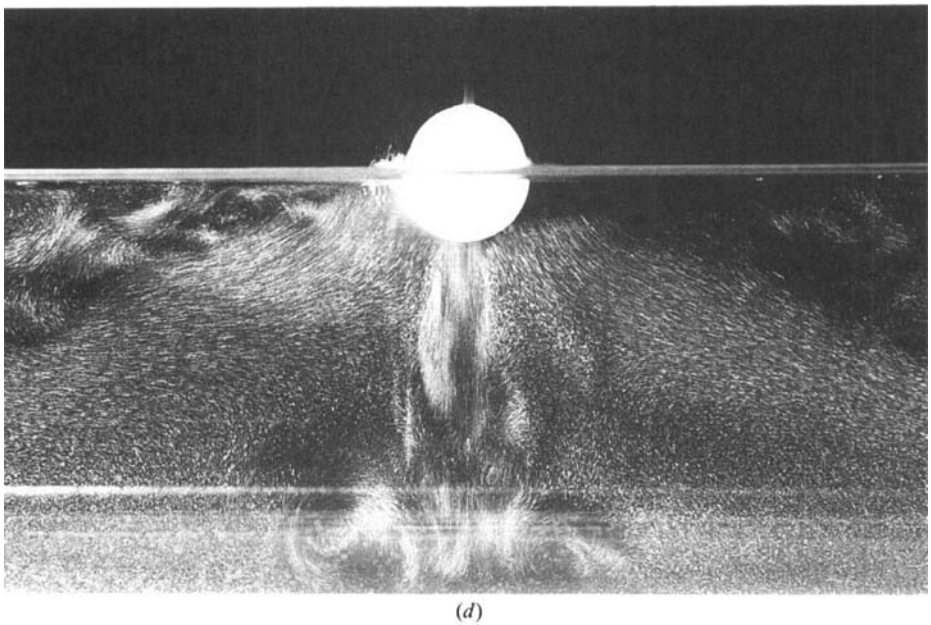

(d)

FIGURE 5. Vertical jet flows: (a) = 0.64 mm; (b) 0.81 mm; (c) 1.10 mm; (d) 2.00 mm. (Time of exposure is 1 s; elapsed time from initiation of the sphere's oscillation is 30 s.)

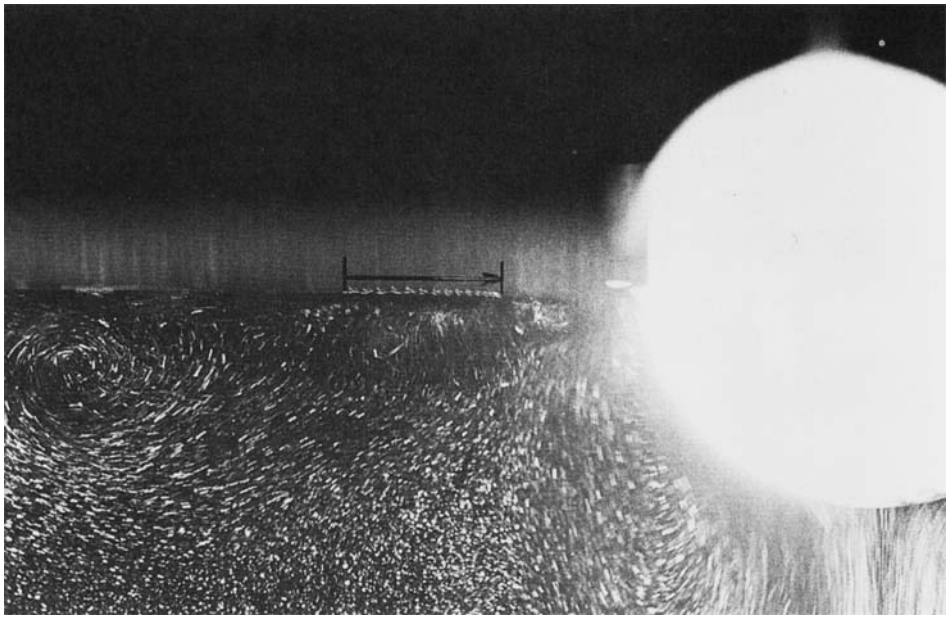

FIGURE 6. Closeup of the flow in a central vertical section. ($a = 0.75$ mm; time of exposure is 1 s; elapsed time from initiation of the sphere's oscillation is 30 s; the arrow shows the movement of a small air bubble on the water surface.)

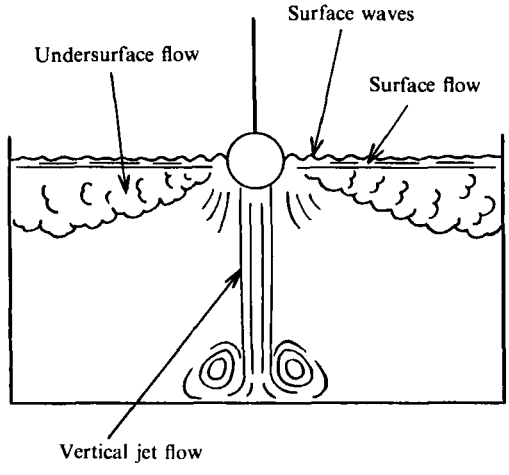

FIGURE 7. Sketch of the flow structure.

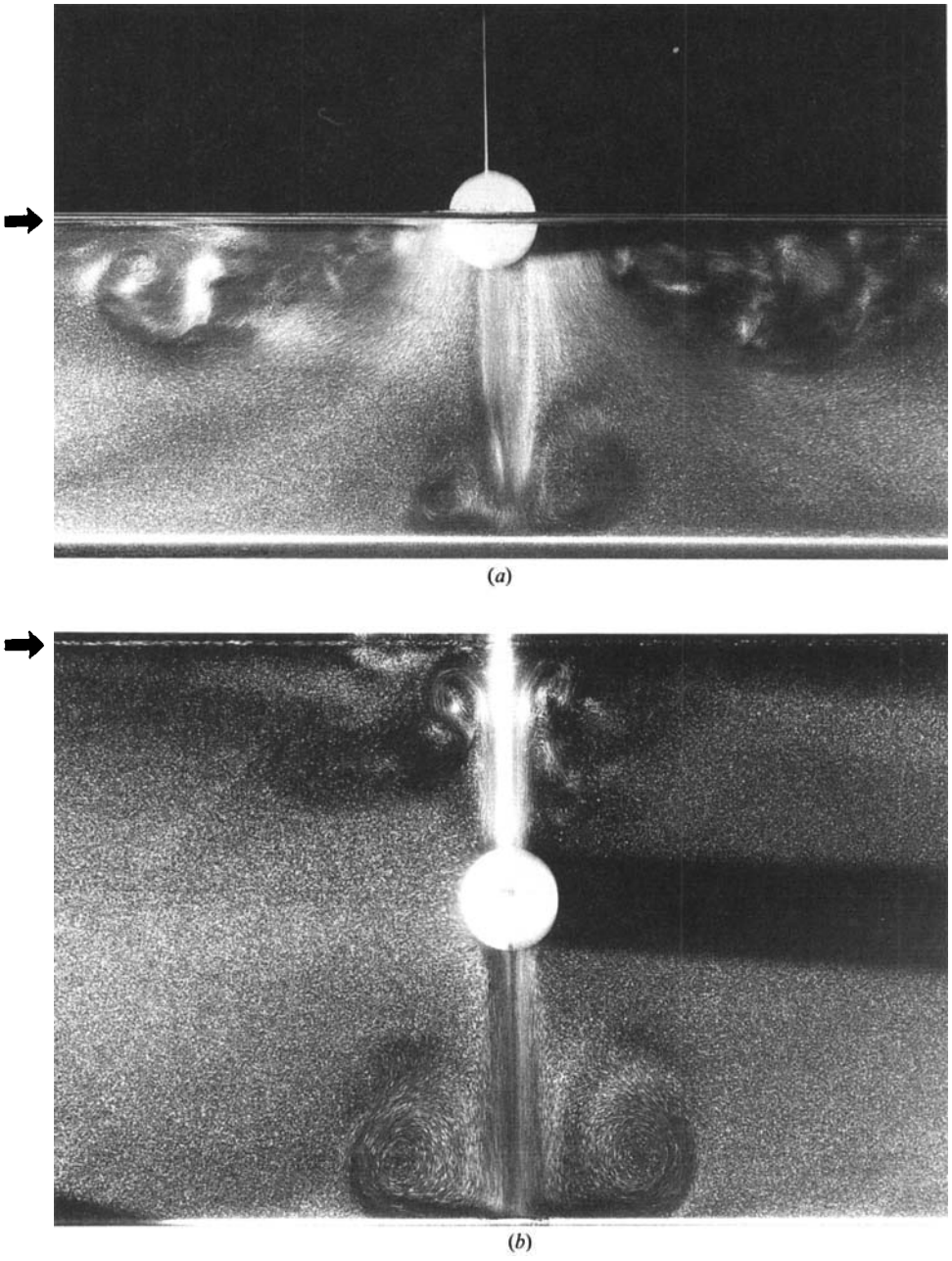

FIGURE 8. Comparison of the flow around a half-submerged oscillating sphere (*a*) and the flow around a completely submerged oscillating sphere (*b*). ($a = 1.55$ mm; time of exposure is 1 s; elapsed time from initiation of the sphere's oscillation is 30 s; the arrows indicate the surface of the water.)

that the velocity of the undersurface flow is much smaller than that of the surface flow, and that the thickness of the surface flow is extremely small.

Figure 7 shows a sketch of the flow structure around a half-submerged oscillating sphere in the case when the petal-shaped waves are generated on the water surface.

Figure 8 shows a comparison of the flow around a half-submerged sphere (figure 8*a*), with the flow around a fully submerged sphere at the same oscillation amplitude (figure 8*b*). In the case of a completely submerged sphere (figure 8*b*), the depth of the water is 26 cm. It is readily seen that in the case when the sphere is completely submerged, only the vertical jet flow occurs.

4. Discussion

The concentric circular waves which appear at small oscillation amplitudes (figure 2*a*) are well described with the classical linear theory. The observed wave velocity is in good agreement with the theoretically calculated one. The period-doubling bifurcation which can be seen in figure 2(*b*) is very interesting both in itself and as a precursor to the fully chaotic behaviour that has emerged when conditions attain those of figure 2(*f*).

The present experiments show that the surface and undersurface flows are generated only when the petal-shaped waves occur on the water surface. This suggests that the surface and undersurface flows are induced by the action of the petal-shaped waves. It should be noted here that there are other surface-limited flows which are generated by surface wave interactions, namely Langmuir circulations (see, for example, Langmuir 1938; Craik & Leibovich 1976; Garrett 1976).

As will be seen from figures 8(*a*) and 8(*b*), whether the sphere is half-submerged or fully submerged, the jet-like flows are generated in the same manner. This suggests that the vertical jet flow is independent of the surface waves. There is a considerable literature on the 'streaming' which is generated around a fully submerged oscillating body (see, for example, Lane 1955; Davidson & Riley 1972; Bertelsen 1974; Riley 1975; Amin & Riley 1990; Tatsuno & Bearman 1990).

The flow structure around a half-submerged oscillating sphere is thought to depend on ρ, ν, d, a, f, g, and T, where ρ is the density of the fluid, ν its kinematic viscosity, d the sphere diameter, a its oscillation amplitude, f its frequency, g the gravitational acceleration, and T the surface tension. Therefore, the flow structure is expected to be governed by four dimensionless parameters: a/d, fd^2/ν, af^2/g, and $\rho d^3f^2/T$. Further systematic experiments on the variation of the flow structure with the dimensionless parameter are being carried out.

REFERENCES

Amin, N. & Riley, N. 1990 *J. Fluid Mech.* **210**, 459.

Bertelsen, A. F. 1974 *J. Fluid Mech.* **64**, 589.

Craik, A. D. D. & Leibovich, S. 1976 *J. Fluid Mech.* **73**, 401.

Davidson, B. J. & Riley, N. 1972 *J. Fluid Mech.* **53**, 287.

Garrett, C. J. R. 1976 *J. Mar. Res.* **34**, 117.

Lane, C. A. 1955 *J. Acoust. Soc. Am.* **2**, 1082.

Langmuir, I. 1938 *Science* **87**, 119.

Okabe, J. & Inoue, S. 1967 *Bull. Res. Inst. Appl. Mech.* **26**, 99.

Riley, N. 1975 *J. Fluid Mech.* **68**, 801.

Taneda, S. 1986 *Fluid Dyn. Res.* **1**, 1.

Tatsuno, M. & Bearman, P. W. 1990 *J. Fluid Mech.* **211**, 157.

Tatsuno, M., Inoue, S. & Okabe, J. 1969 *Rep. Res. Inst. Appl. Mech.* **17**, 195.